

Molybdenum-Catalyzed Transformation of Molecular Dinitrogen into Silylamine: Experimental and DFT Study on the Remarkable Role of Ferrocenyldiphosphine Ligands

Hiromasa Tanaka,[†] Akira Sasada,[†] Tomohisa Kouno,[†] Masahiro Yuki,[‡] Yoshihiro Miyake,[‡] Haruyuki Nakanishi,[§] Yoshiaki Nishibayashi,^{*,‡} and Kazunari Yoshizawa^{*,†}

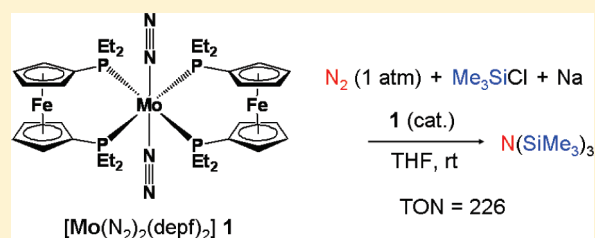
[†]Institute for Materials Chemistry and Engineering, Kyushu University, Nishi-ku, Fukuoka, Fukuoka 819-0395, Japan

[‡]Institute of Engineering Innovation, School of Engineering, The University of Tokyo, Yayoi, Bunkyo-ku, Tokyo 113-8656, Japan

[§]Fuel Cell System Development Center, Toyota Motor Corporation, Mishuku, Susono, Shizuoka 410-1193, Japan

S Supporting Information

ABSTRACT: A molybdenum–dinitrogen complex bearing two ancillary ferrocenyldiphosphine ligands, *trans*-[Mo(N₂)₂(depf)₂] (depf = 1,1'-bis(diethylphosphino)ferrocene), catalyzes the conversion of molecular dinitrogen (N₂) into silylamine (N(SiMe₃)₃), which can be readily converted into NH₃ by acid treatment. The conversion has been achieved in the presence of Me₃SiCl and Na at room temperature with a turnover number (TON) of 226 for the N(SiMe₃)₃ generation for 200 h. This TON is significantly improved relative to those ever reported by Hidai's group for mononuclear molybdenum complexes having monophosphine coligands [*J. Am. Chem. Soc.* **1989**, *111*, 1939]. Density functional theory (DFT) calculations have been performed to figure out the mechanism of the catalytic N₂ conversion. On the basis of some pieces of experimental information, SiMe₃ radical is assumed to serve as an active species in the catalytic cycle. Calculated results also support that SiMe₃ radical is capable of working as an active species. The formation of five-coordinate intermediates, in which one of the N₂ ligands or one of the Mo–P bonds is dissociated, is essential in an early stage of the N₂ conversion. The SiMe₃ addition to a “hydrazido(2–)” intermediate having the NN(SiMe₃)₂ group will give a “hydrazido(1–)” intermediate having the (Me₃Si)NN(SiMe₃)₂ group rather than a pair of a nitrido (≡N) intermediate and N(SiMe₃)₃. The N(SiMe₃)₃ generation would not occur at the Mo center but proceed after the (Me₃Si)NN(SiMe₃)₂ group is released from the Mo center. The flexibility of the Mo–P bond between Mo and depf would play a vital role in the high catalysis of the Mo–Fe complex.



INTRODUCTION

Nitrogen fixation under ambient reaction conditions is one of the most important and challenging topics in chemistry.¹ Molecular dinitrogen (N₂) is chemically inert due to its extremely strong, nonpolar triple bond (225 kcal/mol) as well as the large HOMO–LUMO gap. Industrial nitrogen fixation typified by the Haber–Bosch process requires drastic reaction conditions of high pressures and high temperatures. Since the discovery of the first transition metal–N₂ complex [Ru(N₂)(NH₃)₅]²⁺ by Allen and Senoff in 1965,² a great deal of effort has been devoted to the development of artificial nitrogen fixation systems that are capable of working under mild reaction conditions. Nowadays, a great number of well-defined N₂ complexes are known for almost all d-block transition metals as well as some f-block metals, and a lot of studies have been reported so far on stoichiometric transformation of their coordinated N₂ into ammonia (NH₃) and hydrazine (NH₂NH₂).^{3–14} In 1975, for example, Chatt and co-workers found the formation of NH₃ by protonolysis of tungsten–N₂ and molybdenum–N₂ complexes [M(N₂)₂(PR₃)₄] (M = Mo, W).¹⁵ In sharp contrast to such stoichiometric reactivity of transition-metal–N₂ complexes, there are only a few examples of the catalytic

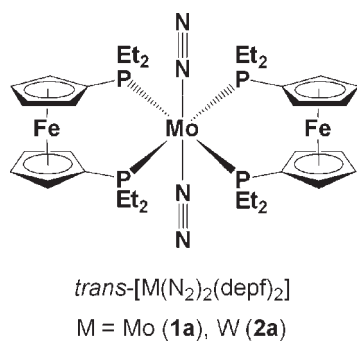
transformation of N₂ into NH₃ and/or its NH₃ equivalent using transition metal complexes under mild reaction conditions.¹⁶ In 1972, Shiina discovered the metal-chloride-catalyzed reductive transformation of N₂ into tris(trimethylsilyl)amine (N(SiMe₃)₃), which can be readily converted into NH₃ by acid treatment, in the presence of Me₃SiCl and lithium.¹⁷ The turnover number (TON) of N(SiMe₃)₃ generation was up to 5.4 (CrCl₃). Hidai, Mizobe, and co-workers reported in 1989 a more effective method for N(SiMe₃)₃ generation using Me₃SiCl and sodium together with molybdenum–N₂ complexes such as [Mo(N₂)₂(PMe₂Ph)₄] as a catalyst.¹⁸ In their reaction system, the TON reached 24 based on the Mo atom. The mechanism of this catalytic reaction still remains to be elucidated although they proposed a mechanism involving a silyldiazenido intermediate formed by the attack of SiMe₃ radical on the N₂ ligand. Recently, Yandulov and Schrock reported the direct conversion of N₂ into NH₃ using a molybdenum–N₂ complex bearing an ancillary triamidoamine ligand.¹⁹ They adopted a pair of proton and electron

Received: October 19, 2010

Published: February 22, 2011

donors, lutidinium and decamethylchromocene, for the nitrogen fixation and proposed a catalytic mechanism containing successive hydrogenation of N_2 through alternating steps of protonation and reduction. The hydrogenation of a $Mo-NNH_2$ intermediate gives a nitrido ($\equiv N$) intermediate and the first molecule of NH_3 , and then the nitrido ligand on Mo is converted into the second molecule of NH_3 . At present, the validity of this mechanism is strongly supported by the isolation and observation of a large part of reactive intermediates as well as intensive theoretical studies on the catalytic cycle.^{20–24} Unfortunately, the TON for the NH_3 generation was not very high (up to 8 based on the Mo atom).²⁵

Quite recently, some of us have reported the synthesis and the stoichiometric reactivity of molybdenum– N_2 and tungsten– N_2 complexes bearing ferrocenyldiphosphines as auxiliary ligands, *trans*- $[M(N_2)_2(depf)_2]$ ($M = Mo$ (**1a**), W (**2a**); *depf* = 1,1'-bis(diethylphosphino)ferrocene), where the electron transfer process from the ferrocene moiety to the tungsten or molybdenum center may be expected to assist the reduction of the coordinated N_2 into NH_3 .²⁶ During the continuous study on the development of novel nitrogen fixation system under mild reaction conditions,²⁷ a more efficient catalytic nitrogen fixation system was found by using **1a** as a catalyst. Dinitrogen under an atmospheric pressure was catalytically converted into $N(SiMe_3)_3$ in the presence of Me_3SiCl and sodium in quite a high TON.

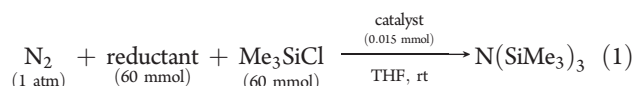


An intriguing subject is to elucidate how the coordinated N_2 is converted in this multimetallic system and how the *depf* ligands enhanced the catalysis for the conversion of N_2 into $N(SiMe_3)_3$. For the present reaction system, unfortunately, we have not obtained

experimental information that can be directly associated with the determination of the catalytic mechanism. Computational quantum chemistry will provide a valuable insight into our understanding. Actually, some of us have computationally revealed the mechanisms on the activation and triple-bond cleavage of N_2 by a cubane-type $RuIr_3S_4$ cluster²⁸ as well as a hydride-bridged dinobium complex.²⁹ In this Article, we describe typical results of the catalytic conversion of N_2 into $N(SiMe_3)_3$ using **1a** as a catalyst and propose a possible reaction pathway by quantum chemical calculations.

RESULTS AND DISCUSSION

Catalytic Conversion of N_2 into $N(SiMe_3)_3$ by **1a.** Typical experimental results are summarized in Table 1 for the conversion of N_2 into $N(SiMe_3)_3$ by using **1a** as a catalyst. Details are described in the Supporting Information. Treatment of Na (60 mmol) and Me_3SiCl (60 mmol) in the presence of a catalytic amount of **1a** (0.015 mmol) in THF (tetrahydrofuran; 40 mL) under an atmospheric pressure of N_2 at room temperature for 20 h gave 1.35 mmol of $N(SiMe_3)_3$ together with some side products such as $Me_3SiSiMe_3$, $Me_3Si(CH_2)_4OSiMe_3$, and tBuOSiMe_3 (eq 1; Table 1, run 1). The generated $N(SiMe_3)_3$ was isolated from the reaction mixture and confirmed by 1H and ${}^{13}C$ NMR and MS.



The amounts of $N(SiMe_3)_3$ and other side-products were determined by GLC analysis. The TON for the formation of $N(SiMe_3)_3$ was 90 based on the Mo atom of **1a**. A longer reaction time (100 h) increased the amount of $N(SiMe_3)_3$ up to 1.77 mmol, corresponding to a TON of 118 (Table 1, run 2). In the reaction with Li as a reductant in place of Na (Table 1, run 3) for 100 h, a smaller amount of $N(SiMe_3)_3$ (0.56 mmol, TON = 37) was formed together with a larger amount of $Me_3SiSiMe_3$ (16.53 mmol). The reaction in a more dilute solution (60 mL of THF) yielded a larger amount of $N(SiMe_3)_3$ (2.25 mmol, TON = 150; Table 1, run 4) than the result of run 2 of Table 1. The TON reached 184 after 150 h, and Me_3SiCl was confirmed to be depleted in the reaction solution (Table 1, run 5). Here, we considered that the presence of more Na and Me_3SiCl may produce an extra amount of $N(SiMe_3)_3$ from the reaction mixture

Table 1. Reactions Using Reductant (60 mmol) and Me_3SiCl (60 mmol) Were Carried Out in the Presence of a Catalyst (0.015 mmol) under Atmospheric Pressure of N_2 at Room Temperature in THF

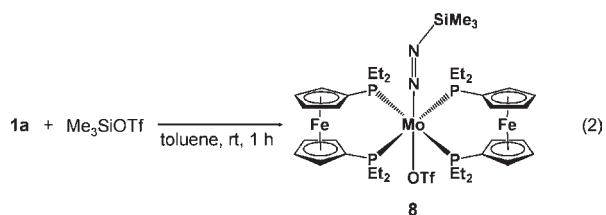
run	catalyst	reductant	THF (mL)	time (h)	amount of $N(SiMe_3)_3$ (mmol) ^a	TON ^b
1	1a	Na	40	20	1.35	90
2	1a	Na	40	100	1.77	118
3	1a	Li	40	100	0.55	37
4	1a	Na	60	100	2.25	150
5 ^c	1a	Na	60	200	3.39	226
6	3	Na	40	20	0.48	32
7	1b	Na	40	20	0.81	54
8	4	Na	40	20	0.01	<1
9	2a	Na	40	20	0.90	60
10	5	Na	40	20	0.24	16
11	6	Na	40	20	0.18	12
12	7	Na	40	20	0.04	3
13	8	Na	40	20	0.66	44

^a Determined by GLC. ^b TON = $N(SiMe_3)_3$ /catalyst. ^c Another THF solution (60 mL) of Me_3SiCl (60 mmol) and Na (60 mmol) was added after 100 h.

when the catalytic ability of **1a** is still alive at this stage. In fact, addition of Na (60 mmol) and Me₃SiCl (60 mmol) to the reaction solution after 100 h produced an extra amount of N(SiMe₃)₃ from the solution used in reaction mixture. The total amount of N(SiMe₃)₃ was finally measured to be 3.39 mmol with a TON of 226 (Table 1, run 5). Both N₂ gas and **1a** were confirmed to be indispensable for the formation of N(SiMe₃)₃ (see the Supporting Information).

Under the reaction conditions similar to run 1 in Table 1, replacement of **1a** with *trans*-[Mo(N₂)₂(depf)(PMePh₂)₂] (**1b**) and *cis*-[Mo(N₂)₂(PMe₂Ph)₄] (**3**) decreased the TONs to 54 and 32, respectively (Table 1, runs 6 and 7). Previously, Hidai's group reported that *cis*-[W(N₂)₂(PMe₂Ph)₄] (**4**) did not work as a catalyst for the formation of N(SiMe₃)₃.¹⁸ We also confirmed that **4** did not catalyze this reaction under the same reaction conditions (Table 1, run 8). Interestingly, the reaction in the presence of a catalytic amount of *trans*-[W(N₂)₂(depf)₂] (**2a**) gave N(SiMe₃)₃, where the TON reached 60 (Table 1, run 9). In sharp contrast to the efficient catalysis of **1a** and **2a**, low catalysis was observed for molybdenum–N₂ and tungsten–N₂ complexes having other diphosphines as ancillary ligands such as *trans*-[Mo(N₂)₂(dppe)₂] (dppe = 1,2-bis(diphenylphosphino)ethane; **5**), *trans*-[Mo(N₂)₂(depe)₂] (depe = 1,2-bis(diethylphosphino)ethane; **6**), and *trans*-[W(N₂)₂(depr)₂] (depr = 1,1'-bis(diethylphosphino)ruthenocene; **7**). The TONs for the N(SiMe₃)₃ formation were measured to be 16 for **5**, 12 for **6**, and 3 for **7** (Table 1, runs 10–12). All the experimental results clearly show that the depf ligands in **1a** and **2a** are responsible for their efficient catalysis. Unfortunately, we were not able to detect any structurally defined complexes by NMR after the catalytic reaction. As a piece of experimental information leading to elucidation of the catalytic mechanism, it should be noted that N(SiMe₃)₃ was not observed at all when dry air was used in place of N₂. This would imply that O₂ in the air inhibited the generation of radical species such as SiMe₃ radical.

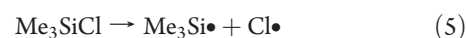
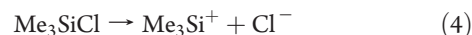
Previously, Hidai's group reported the synthesis of a series of silyldiazenido complexes by the reaction of Mo and W dinitrogen complexes such as **3**, **4**, and **5** with Me₃SiI, Me₃SiCl/NaI, or Me₃SiOTf. It was further revealed that reduction of *trans*-[M(NNSiMe₃)(PMe₂Ph)₄] (M = Mo, W) with Na in the presence of Me₃SiCl under Ar affords N(SiMe₃)₃ as a principal nitrogenous product.^{18,34} We investigated the stoichiometric reaction of **1a** with 1 equiv of Me₃SiOTf (OTf = OSO₂CF₃) at room temperature for 1 h, which gave the corresponding silyldiazenido complex (**8**) in 69% isolated yield (eq 2). When **8** was used as a catalyst in place of **1a**, the TON for N(SiMe₃)₃ was 44 (Table 1, run 13). In addition, the stoichiometric reaction of **8** with Na (20 equiv) and Me₃SiCl (20 equiv) under an atmospheric pressure of argon afforded N(SiMe₃)₃ in 88% yield based on **8** (eq 3). These results suggest that the diazenido complex **8** can be regarded as a reactive intermediate in the catalytic formation of N(SiMe₃)₃.



Theoretical Calculations. In this section, we describe a theoretical study on a mechanism of the conversion of N₂ into

N(SiMe₃)₃ catalyzed **1a**. We briefly discuss the active silyl species in the reaction solution and then propose a plausible mechanism of the catalytic N₂ conversion. All calculations were carried out by using the Gaussian09 program package.³⁰ All intermediates proposed in this study were searched on potential energy surfaces by using the hybrid density functional B3LYP method.³¹ For optimization, the LANL2DZ and 6-31G(d) basis sets were chosen for the metal atoms (Mo, Fe) and the other atoms, respectively (BS1).³² Optimized structures were confirmed to have no imaginary frequencies by vibrational analyses. Ancillary depf ligands were included without any simplification. The total charge of **1a** is equal to 0, and thus, the formal charges of Mo and Fe in **1a** are 0 and +2, respectively. To determine the energy profile of the proposed catalytic cycle, we performed single-point calculations at the optimized geometries using the 6-311+G(d) basis set instead of the 6-31G(d) basis set (BS2). Solvation effects (THF) were taken into account by using the polarizable continuum model (PCM).³³ Zero-point energy corrections were applied for enthalpy changes (ΔH₀) and activation energies (E_a) calculated for each reaction step.

1. Active Silyl Species. As mentioned above, SiMe₃ radical is a possible active silyl species in the present reaction system. Here we would like to deduce the active silyl species based on theoretical calculations. If the active silyl species is directly generated by the Si–Cl bond cleavage of Me₃SiCl, the heterolysis of Me₃SiCl gives SiMe₃⁺ and Cl[−] (eq 4), while the homolysis gives a pair of SiMe₃ and Cl radicals (eq 5):



The Si–Cl bond energy in THF is calculated to be 70.2 kcal/mol for the heterolysis and 107.3 kcal/mol for the homolysis at the B3LYP/6-311+G(d) level of theory. The large Si–Cl bond energies for both the homolysis and heterolysis indicate that a neutral Me₃SiCl molecule would give neither SiMe₃ cation nor SiMe₃ radical at room temperature. We can therefore rule out a reaction mechanism containing “alternative protonation/reduction steps” from consideration, which is commonly accepted for nitrogen fixation catalyzed by Schrock's Mo complex.^{19–24}

Here we consider the role of sodium in the reaction mixture. If sodium in the reaction solution reduces Me₃SiCl in advance, the generated Me₃SiCl[−] anion is readily cleaved into SiMe₃ radical and Cl anion (eqs 6 and 7):



From the difference in energy between the optimized structures of Me₃SiCl and Me₃SiCl[−], the adiabatic electron affinity of Me₃SiCl is calculated to be −13.2 kcal/mol. The Si–Cl bond cleavage of Me₃SiCl[−] in THF is *exergonic* by 7.3 kcal/mol. These values are in good agreement with the experimental fact that Me₃SiCl molecules slowly generate disilane Me₃SiSiMe₃ in the presence of Na in THF. From both the experimental and theoretical results, the following discussion focuses on a radical mechanism in which SiMe₃ radical plays a role in the catalysis.

2. Catalytic Mechanism for the Dinitrogen-to-Silylamine Conversion. We present in Figure 1 a plausible mechanism on the conversion of N₂ into N(SiMe₃)₃ via successive addition of

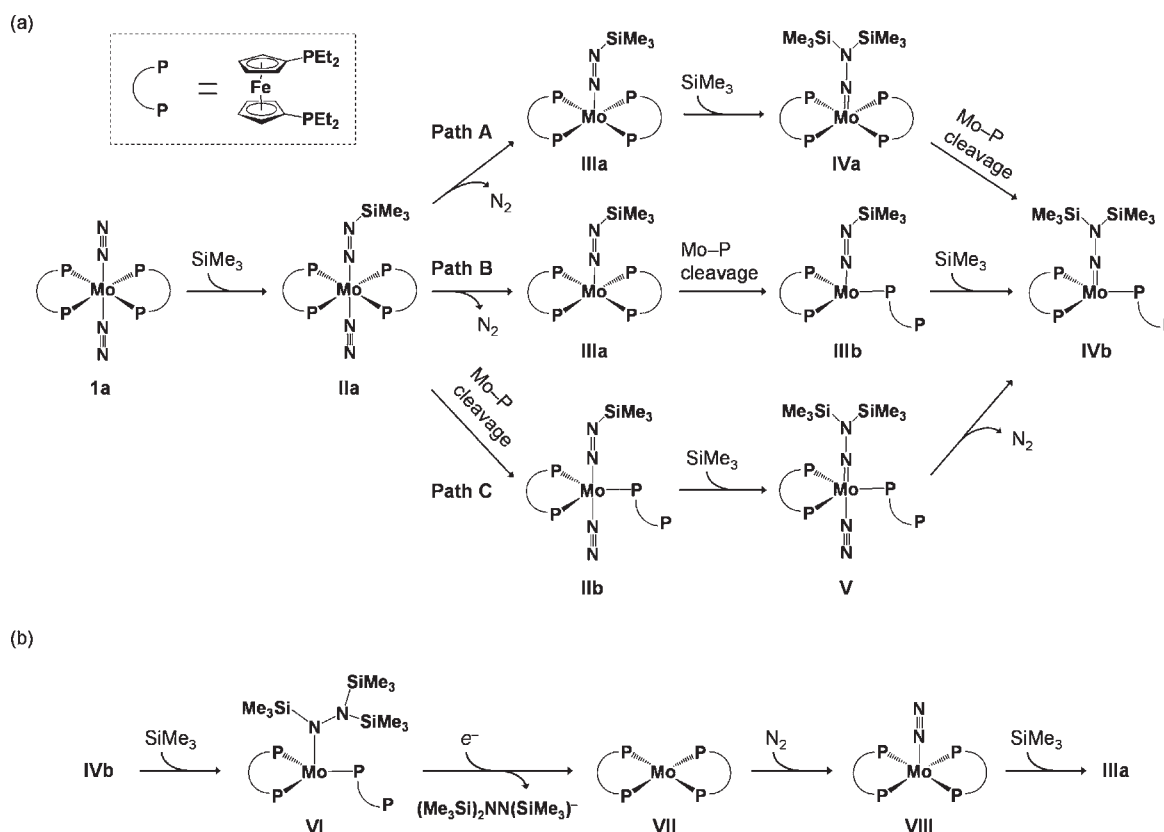


Figure 1. Possible mechanism of the catalytic conversion of N_2 into $\text{N}(\text{SiMe}_3)_3$ by a molybdenum complex bearing ferrocenyldiphosphines. (a) Three pathways to yield the four-coordinate intermediate **IVb**. (b) The formation of $(\text{Me}_3\text{Si})_2\text{NN}(\text{SiMe}_3)$ anion and the start of the next catalytic cycle. SiMe_3 represents trimethylsilyl radical.

SiMe_3 radicals, which is partially relevant to Hidai and Mizobe's proposal for $\text{cis-}[\text{Mo}(\text{N}_2)_2(\text{PMe}_2\text{Ph})_4]$ **3**.³⁴ In their catalytic mechanism, a five-coordinate intermediate is first formed by the dissociation of one N_2 ligand in **3**. Figure 2 shows optimized structures of **1a** and intermediates **II–VIII** proposed in the present calculation. Figure 3 shows the overall energy profile containing the enthalpy change and activation energy (in parentheses) for each reaction step. Detailed information on the reaction steps, such as optimized structures of reactant complexes, transition states, and product complexes, are described in the Supporting Information. The conversion starts with the addition of SiMe_3 to one of the N_2 ligands in **1a** to yield $[\text{Mo}(\text{N}_2)(\text{NNSiMe}_3)(\text{depf})_2]$ **IIa**. There are three possible pathways (paths A–C) leading to the doubly silylated intermediate **IVb** having the $\text{NN}(\text{SiMe}_3)_2$ group. In paths A and B, **IIa** releases the N_2 ligand to form a five-coordinate intermediate $[\text{Mo}(\text{NNSiMe}_3)(\text{depf})_2]$ **IIIa**. In path C, on the other hand, one of the four Mo-P bonds in **IIa** is cleaved to form another five-coordinate intermediate **IIb**. In path A, the second SiMe_3 radical attacks **IIIa** to yield a five-coordinate intermediate **IVa** having the $\text{NN}(\text{SiMe}_3)_2$ group, and then one of the Mo-P bonds in **IVa** is cleaved to give a four-coordinate intermediate **IVb**. In path B, one of the Mo-P bonds in **IIIa** is cleaved in advance, and then the generated four-coordinate intermediate **IIIb** is attacked by the second SiMe_3 radical for the formation of **IVb**. In path C, the five-coordinate **IIb** accepts the second SiMe_3 radical to form $[\text{Mo}(\text{N}_2)(\text{NN}(\text{SiMe}_3)_2)(\text{depf})_2]$ **V**. The N_2 ligand in **V** is then dissociated to give **IVb**. The third SiMe_3 radical attacks the N atom adjacent to the Mo atom of **IVb**, leading to **VI** having the $\text{Me}_3\text{SiNN}(\text{SiMe}_3)_2$ group. One-electron reduction and the Mo-N

bond cleavage of **VI** result in the formation of $[\text{Mo}(\text{depf})_2]$ **VII** and $(\text{Me}_3\text{Si})_2\text{NN}(\text{SiMe}_3)$ anion. This anion liberated into the reaction solution would be readily converted into two molecules of $\text{N}(\text{SiMe}_3)_3$ by Me_3SiCl and SiMe_3 radicals. The next cycle of the conversion of N_2 starts with the binding of a new N_2 molecule by **VII**. The addition of SiMe_3 radical to $[\text{Mo}(\text{N}_2)(\text{depf})_2]$ **VIII** gives **IIIa** and the following reactions proceed along path A or B.

3. Addition of first SiMe_3 Radical and Formation of Five-Coordinate Intermediates. As shown in Figures 1 and 3, the catalytic cycle starts with the addition of SiMe_3 radical to the initial complex **1a**, which is exergonic by 2.6 kcal/mol in THF. The calculated activation barrier (8.3 kcal/mol) is low enough to overcome at room temperature. As mentioned above, there are three possible reaction pathways for the formation of five-coordinate intermediates from the generated intermediate **IIa**: the Mo-N_2 bond dissociation leading to **IIIa** (paths A and B) and the Mo-P bond dissociation leading to **IIb** (path C). As shown in Figure 3, the enthalpy change for the Mo-N_2 bond dissociation of **IIa** (**IIa** \rightarrow **IIIa**) is calculated to be +2.4 kcal/mol ($E_a = 13.7$ kcal/mol) in THF, which is much smaller than that for the Mo-N_2 bond dissociation of **1a** (+18.4 kcal/mol; $E_a = 20.0$ kcal/mol). These values suggest that the silylation of one N_2 ligand prompts the dissociation of the other N_2 ligand. In the Mo-depf system, a five-coordinate intermediate will be formed after the silylation of the initial complex, while the catalytic mechanism proposed for $\text{cis-}[\text{Mo}(\text{N}_2)_2(\text{PMe}_2\text{Ph})_4]$ **3** supposed that one N_2 ligand dissociates from **3** before the addition of SiMe_3 .²⁰

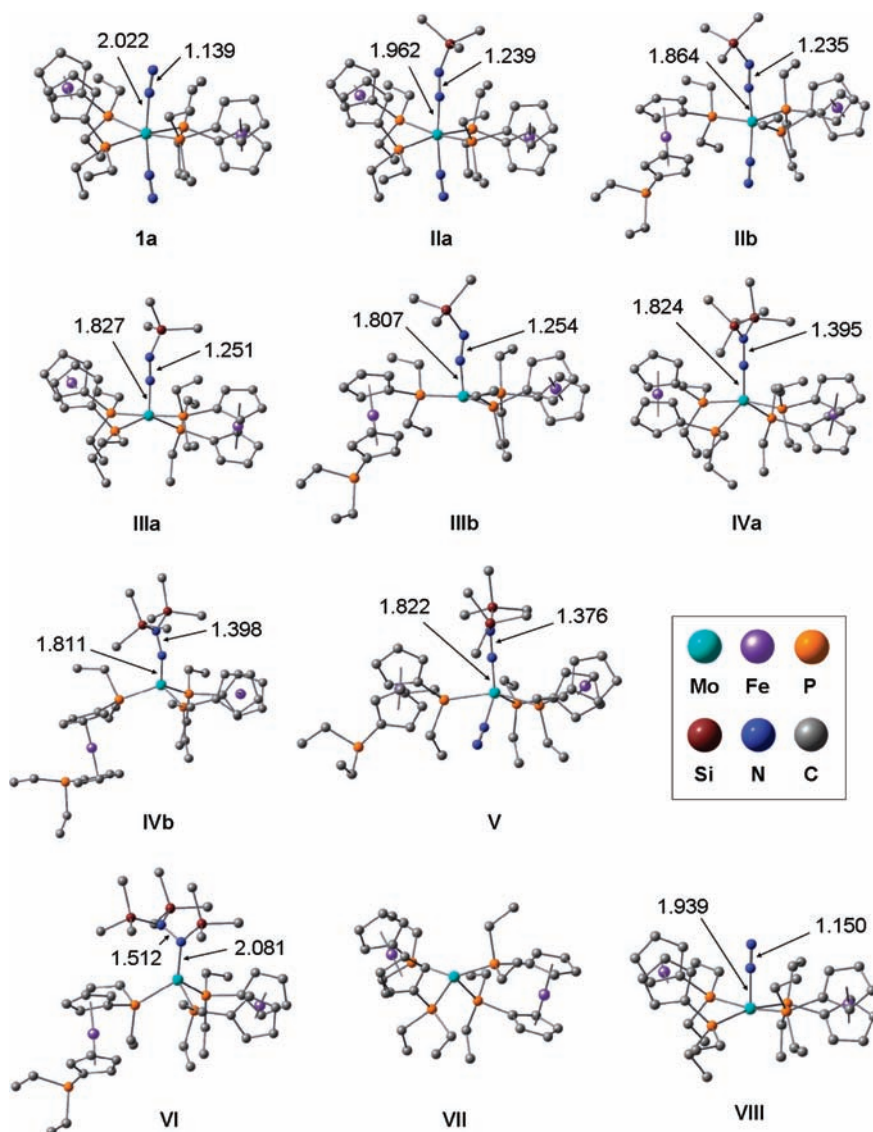


Figure 2. Optimized structures of **1a** and possible intermediates **II–VIII**. Hydrogen atoms are omitted for clarity. Interatomic distances are presented in Å.

Figure 4 presents computed energy changes of **1a** and **IIa** plotted as a function of one of the Mo–P bond distances r . Optimization at each fixed r was carried out at the B3LYP/BS1 level of theory, and the total energy in THF was obtained with a single-point calculation at the B3LYP/BS2 level of theory. For comparison, we show in this figure energy changes calculated for *trans*-[Mo(N₂)₂(dppe)₂] **5** having bidentate phosphine coligands and its silylated complex *trans*-[Mo(N₂)(NNSiMe₃)(dppe)₂] **9**. The Mo–P bond cleavage of **1a** requires E_a of 9.8 kcal/mol, and the corresponding five-coordinate structure (Mo–P = 6.371 Å) is 6.0 kcal/mol less stable than **1a**. The activation energy for the Mo–P cleavage of **5** is calculated to be much higher (18.7 kcal/mol), and the five-coordinate structure (Mo–P = 5.205 Å) is 16.8 kcal/mol less stable than the six-coordinate structure. On the other hand, the silylation of **1a** makes a five-coordinate structure energetically more favorable, probably due to the steric repulsion between the SiMe₃ group and the bulky depf ligand; the five-coordinate intermediate **IIb** (Mo–P = 6.876 Å) is 8.5 kcal/mol more stable than **IIa**, and E_a for the Mo–P bond cleavage is only 2.5 kcal/mol. Contrary to

IIa, the five-coordinate structure of **9** (Mo–P = 5.885 Å) is 1.8 kcal/mol less stable than the six-coordinate one and E_a (8.4 kcal/mol) is much higher than that of **IIa**. If the catalytic formation of N(SiMe₃)₃ by **5** proceeds in a similar manner to **1a**, high catalytic ability of **1a** relative to **5** may be explained by facile Mo–P bond cleavage in **IIa** as well as the higher thermodynamic stability of the five-coordinate **IIb** than the six-coordinate **IIa**. This is because one of the Mo–P bonds or the Mo–N₂ bond must be dissociated before accepting the second SiMe₃ radical, as mentioned later in subsections 4 and 5.

For the following reaction steps leading to **IVb** having the NN(SiMe₃)₂ group, we consider both pathways that start from **IIIa** and **IIIb**. The addition of SiMe₃ to **IIa** to optimize a “diazene” intermediate having the Me₃SiN=NSiMe₃ group gave the corresponding intermediate having the NN(SiMe₃)₂ group.

4. *Formation of Four-Coordinate IVb via IIIa (Paths A and B).* An intermediate having the NN(SiMe₃)₂ group must dissociate one of the Mo–P bonds to accept the third SiMe₃ radical, and therefore, intermediate **IVb** has a four-coordinate structure. As shown in Figure 1, two reaction pathways are possible to lead

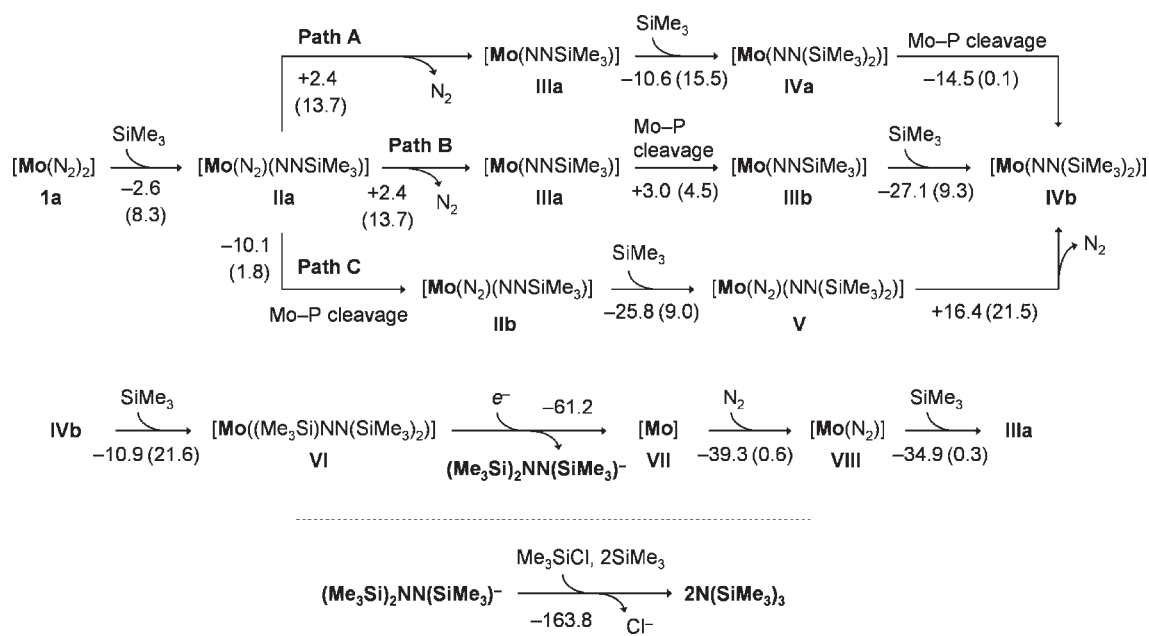


Figure 3. Energy profile of the catalytic conversion of N_2 into $\text{N}(\text{SiMe}_3)_3$ by **1a**. [Mo] and SiMe_3 represent $[\text{Mo}(\text{depf})_2]$ and trimethylsilyl radical, respectively. The enthalpy change ΔH_0 and activation energy (E_a , in parentheses) for each reaction step were calculated at the B3LYP/BS2 level of theory, and solvation effects (THF as a solvent) were taken into account. The energies are presented in kcal/mol.

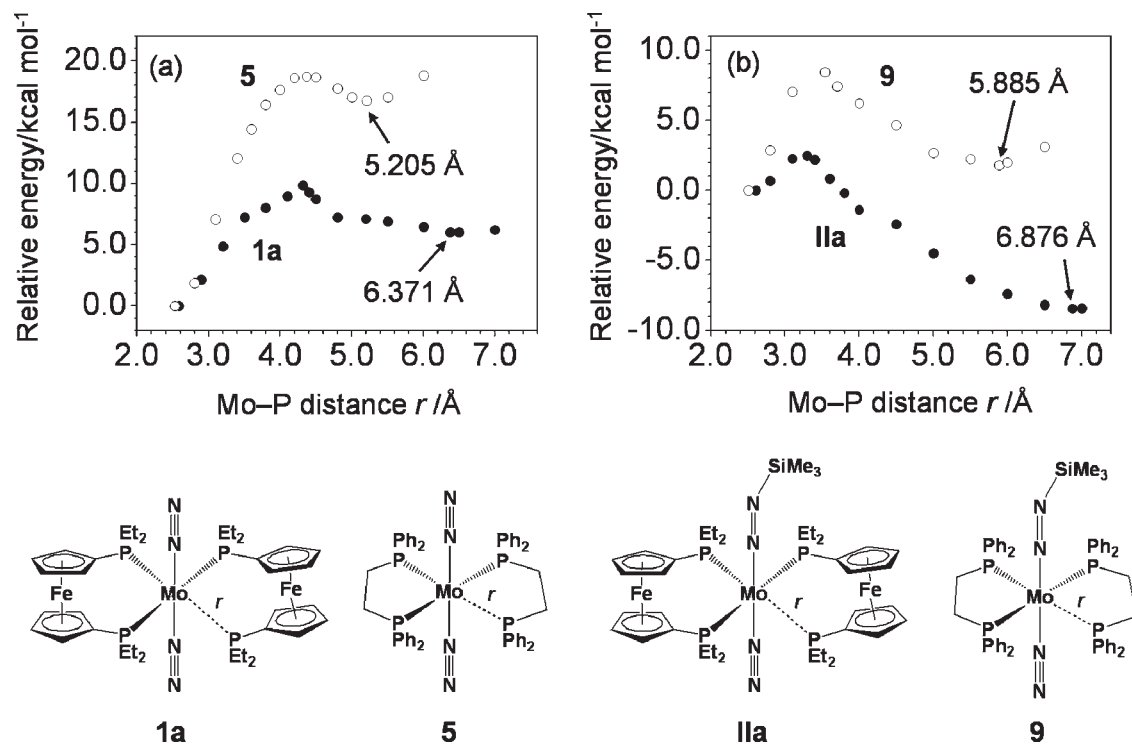


Figure 4. Energy changes for a Mo–P bond cleavage in (a) **1a** and **5** and (b) their silylated complexes **IIa** and **9**. Units are presented in kcal/mol.

to **IVb** from **IIIa**: The addition of SiMe_3 to **IIIa** is followed by the Mo–P bond cleavage (path A; **IIIa** \rightarrow **IVa** \rightarrow **IVb**). In the other pathway, one of the Mo–P bonds in **IIIa** is dissociated in advance, and then SiMe_3 radical attacks to form **IVb** (path B; **IIIa** \rightarrow **IIIb** \rightarrow **IVb**). As shown in Figure 3, the addition of SiMe_3 to **IIIa** yielding **IVa** is calculated to be an exergonic reaction ($\Delta H_0 = -10.6$ kcal/mol) with a moderate E_a (15.5 kcal/mol). The five-coordinate **IVa** having the bulky

$\text{NN}(\text{SiMe}_3)_2$ group readily dissociates one Mo–P bond to give the four-coordinate **IVb** ($\Delta H_0 = -14.5$ kcal/mol, $E_a = 0.1$ kcal/mol). In path B, the Mo–P bond cleavage of **IIIa** proceeds in an endergonic way by 3.0 kcal/mol and is hampered by a low activation barrier (4.5 kcal/mol). Instead, the addition of the second SiMe_3 radical to **IIIb** yielding **IVb** is a highly exergonic reaction ($\Delta H_0 = -27.1$ kcal/mol) with E_a of 9.3 kcal/mol, which is lower than that for **IIIa** \rightarrow **IVa**. The calculated ΔH_0 and E_a values

bond in **VI** ($\text{VI} \rightarrow \text{VII} + \text{Me}_3\text{SiNN}(\text{SiMe}_3)_2$) is +3.9 kcal/mol (endergonic) in THF at the B3LYP/BS2 level of theory, while that for the heterolysis of **VI** ($\text{VI} \rightarrow \text{VII}^+ + \text{Me}_3\text{SiNN}(\text{SiMe}_3)_2^-$) is -52.9 kcal/mol (highly exergonic). The cationic **VII** would be readily neutralized by sodium in the reaction solution because the neutral **VII** is 8.3 kcal/mol energetically more favorable than the cation. There is another reaction pathway that **VI** is reduced by sodium in advance and then the anionic **VI** releases $\text{Me}_3\text{SiNN}(\text{SiMe}_3)_2^-$. The anionic **VI** is 45.5 kcal/mol lower in energy than the neutral **VI**, and the Mo–N bond cleavage of the anionic **VI** is exergonic by 15.7 kcal/mol. In total, the one-electron reduction and Mo–N bond cleavage of **VI** to yield **VII** and $\text{Me}_3\text{SiNN}(\text{SiMe}_3)_2^-$ proceed in an exergonic way by 61.2 kcal/mol. $\text{Me}_3\text{SiNN}(\text{SiMe}_3)_2^-$ liberated into the reaction solution will be converted into two molecules of $\text{N}(\text{SiMe}_3)_3$ by Me_3SiCl and SiMe_3 radicals; the enthalpy change for reaction $\text{Me}_3\text{SiNN}(\text{SiMe}_3)_2^- + \text{Me}_3\text{SiCl} + 2\text{SiMe}_3 \rightarrow 2\text{N}(\text{SiMe}_3)_3 + \text{Cl}^-$ is calculated to be -163.8 kcal/mol in THF. The calculated results suggest that **1a** mediates the conversion of N_2 into $\text{N}(\text{SiMe}_3)_3$ in a different manner from the Yandulov–Schrock mechanism containing a stepwise generation of NH_3 via a nitrido intermediate.¹⁹

7. *Starting the Next Cycle of N_2 Conversion.* As shown in Figures 1 and 3, Intermediate **VII** traps a new N_2 molecule at its Mo center to initiate the next cycle of the N_2 conversion. The binding of N_2 proceeds in an exergonic way ($\Delta H_0 = -39.3$ kcal/mol) as virtually a barrierless reaction ($E_a = 0.6$ kcal/mol). The generated intermediate **VIII** is silylated to form intermediate **IIIa** ($\Delta H_0 = -34.9$ kcal/mol, $E_a = 0.3$ kcal/mol), and the following reaction steps proceed along path A or B. In conclusion, the rate-determining step in all the reaction steps examined here is the addition of the third Si radical to **IVb** yielding intermediate **VI** ($E_a = 21.6$ kcal/mol).

CONCLUSIONS

A molybdenum– N_2 complex bearing ancillary ferrocenyldiphosphine ligands, *trans*- $[\text{Mo}(\text{N}_2)_2(\text{depf})_2]$ **1a**, has catalyzed the conversion of N_2 into $\text{N}(\text{SiMe}_3)_3$ in the presence of Me_3SiCl and Na at room temperature. The turnover number for the $\text{N}(\text{SiMe}_3)_3$ generation finally reached 226 for 200 h, which is greatly improved relative to the precedent molybdenum and tungsten complexes having mono- and diphosphine ligands, such as $[\text{M}(\text{N}_2)_2(\text{PMe}_2\text{Ph})_4]$ and $[\text{M}(\text{N}_2)_2(\text{dppe})_2]$ ($\text{M} = \text{Mo}, \text{W}$).¹⁸ This is so far the most efficient conversion of N_2 into NH_3 equivalent under ambient conditions. With an assumption that SiMe_3 radical works as an active silyl species in the catalytic cycle, we have shown a plausible mechanism of the N_2 conversion by DFT calculations and determined the energy profile of the catalytic cycle from both thermodynamic and kinetic points of view. Almost all of the reaction steps proceed in an exergonic way with reasonably low activation barriers, even the first silylation of N_2 . It is notable that the formation of five-coordinate intermediates is essential in an early stage of the conversion. The first silylation of one N_2 ligand in **1a** prompts bond dissociation between Mo and N_2 as well as Mo and P, while these bonds in **1a** are strong enough to adopt a six-coordinate structure. For the silylation of intermediate **IVb** having the $\text{NN}(\text{SiMe}_3)_2$ group, SiMe_3 radical will not attack the N atom having two SiMe_3 group to form a pair of a nitrido intermediate and $\text{N}(\text{SiMe}_3)_3$ but attack the N atom adjacent to the Mo center to give intermediate **VI** having the $\text{Me}_3\text{SiNN}(\text{SiMe}_3)_2$ group. The $\text{Me}_3\text{SiNN}(\text{SiMe}_3)_2$

group is released from the Mo complex as $\text{Me}_3\text{SiNN}(\text{SiMe}_3)_2^-$ anion and the anion in the reaction solution is readily converted into two molecules of $\text{N}(\text{SiMe}_3)_3$ by Me_3SiCl and SiMe_3 radicals. To afford the $\text{Me}_3\text{SiNN}(\text{SiMe}_3)_2^-$ anion, the Mo–Fe system should be reduced by sodium before or after the Mo–N bond cleavage. Intermediate **VII** traps a single N_2 molecule for starting the next cycle of the $\text{N}(\text{SiMe}_3)_3$ generation. The catalytic mechanism proposed in this study is different from the Yandulov–Schrock mechanism, in which ammonia is generated step-by-step on their Mo complex. The catalysis of **1a** would be sterically controlled by the depf ligands through not only its bulkiness but also the flexible Mo–P bond that allows the Mo center to adopt various coordination numbers. Although we expected that the depf ligands contribute to the high catalysis electronically through an electron transfer from the ferrocene moiety to the Mo center, such theoretical suggestions have not been obtained in the framework of the radical mechanism. For all the intermediates, the Fe atoms in the depf ligands have the formal charge of +2 in their electronic ground states, and the spin state of the ferrocene moieties is always closed-shell singlet. Nevertheless, both the experimental and theoretical results provide convincing evidence that SiMe_3 radical plays a key role in the present reaction system. SiMe_3 cation would not work as an active silyl species because of the presence of a strong reductant (Na) as well as the highly endergonic nature of the heterolysis of Me_3SiCl . We therefore conclude that the radical mechanism presented in this report is highly possible for the catalytic N_2 conversion by **1a**. This conclusion does not necessarily exclude different reaction mechanisms. To reconsider the electronic contribution of the depf ligand to the catalytic ability of **1a**, we are currently investigating a mechanism in which Mo complexes are reduced by Na in place of Me_3SiCl and the anionic Mo species react with the neutral Me_3SiCl .

ASSOCIATED CONTENT

S Supporting Information. Details on experiments, computed energetics, and structural changes in the proposed reaction steps, Cartesian coordinates for all optimized intermediates, and the complete author list of ref 30. This material is available free of charge via the Internet at <http://pubs.acs.org>.

AUTHOR INFORMATION

Corresponding Author

kazunari@ms.ifoc.kyushu-u.ac.jp; ynishiba@sogo.t.u-tokyo.ac.jp

ACKNOWLEDGMENT

K.Y. acknowledges Grants-in-Aid (Nos. 18066013, 18GS0-207, and 22245028) for Scientific Research from Japan Society for the Promotion of Science (JSPS) and the Ministry of Education, Culture, Sports, Science and Technology of Japan (MEXT), the Nanotechnology Support Project of MEXT, the MEXT Project of Integrated Research on Chemical Synthesis, and the Kyushu University Global COE Project for their support of this work. Y.N. acknowledges Grants-in-Aid for Scientific Research for Young Scientists (S) (No. 19675002) and for Scientific Research on Priority Areas (No. 18066003) from MEXT. This paper is dedicated to the late Professor Yasushi Mizobe, Institute of Industrial Science, The University of Tokyo.

REFERENCES

- (1) (a) Ertl, G. In *Catalytic Ammonia Synthesis*; Jennings, J. R., Ed.; Plenum Press: New York, 1991 and references therein. (b) Appl, M. *Ammonia*; Wiley-VCH: Weinheim, 1999 and references therein.
- (2) (a) Allen, A. D.; Senoff, C. V. *Chem. Commun.* **1965**, 621. (b) Bottomley, F.; Nyburg, S. C. *Chem. Commun.* **1966**, 897. (c) Senoff, C. V. *J. Chem. Educ.* **1990**, 67, 368.
- (3) (a) Hidai, M.; Mizobe, Y. *Chem. Rev.* **1995**, 95, 1115. (b) Hidai, M.; Mizobe, Y. *Can. J. Chem.* **2005**, 83, 358.
- (4) (a) Gambarotta, S. *J. Organomet. Chem.* **1995**, 500, 117. (b) Gambarotta, S.; Scott, J. *Angew. Chem., Int. Ed.* **2004**, 43, 5298.
- (5) (a) Fryzuk, M. D.; Johnson, S. A. *Coord. Chem. Rev.* **2000**, 200–202, 379. (b) MacKay, B. A.; Fryzuk, M. D. *Chem. Rev.* **2004**, 104, 385. (c) Fryzuk, M. D. *Acc. Chem. Res.* **2009**, 42, 127. (d) Ballmann, J.; Munhám, S. R. F.; Fryzuk, N. D. *Chem. Commun.* **2010**, 46, 1013.
- (6) Himmel, H.-J.; Reiher, M. *Angew. Chem., Int. Ed.* **2006**, 45, 6264.
- (7) Chirik, P. J. *J. Chem. Soc., Dalton Trans.* **2007**, 16.
- (8) (a) Pool, J. A.; Lobkovsky, E.; Chirik, P. J. *Nature* **2004**, 427, 527. (b) Bart, S. C.; Chłopek, K.; Bill, E.; Bouwkamp, M. W.; Lobkovsky, E.; Neese, F.; Wieghardt, K.; Chirik, P. J. *J. Am. Chem. Soc.* **2006**, 128, 13901. (c) Bart, S. C.; Bowman, A. C.; Lobkovsky, E.; Chirik, P. J. *J. Am. Chem. Soc.* **2007**, 129, 7212. (d) Knobloch, D. J.; Toomey, H. E.; Chirik, P. J. *J. Am. Chem. Soc.* **2008**, 130, 4248. (e) Pun, D.; Bradley, C. A.; Lobkovsky, E.; Keresztes, I.; Chirik, P. J. *J. Am. Chem. Soc.* **2008**, 130, 14046. (f) Pun, D.; Lobkovsky, E.; Chirik, P. J. *J. Am. Chem. Soc.* **2008**, 130, 6047. (g) Knobloch, D. J.; Lobkovsky, E.; Chirik, P. J. *Nat. Chem.* **2010**, 2, 30.
- (9) Gilbertson, J. D.; Szymczak, N. K.; Tyler, D. R. *J. Am. Chem. Soc.* **2005**, 127, 10184.
- (10) (a) Curley, J. J.; Sceats, E. L.; Cummins, C. C. *J. Am. Chem. Soc.* **2006**, 128, 14036. (b) Curley, J. J.; Cook, T. R.; Reece, S. Y.; Müller, P.; Cummins, C. C. *J. Am. Chem. Soc.* **2008**, 130, 9394.
- (11) (a) Evans, W. J.; Lee, D. S.; Ziller, J. W.; Kaltsoyannis, N. *J. Am. Chem. Soc.* **2006**, 128, 14176. (b) Evans, W. J.; Fang, M.; Zucchi, G.; Furche, F.; Ziller, J. W.; Hoekstra, R. M.; Zink, J. I. *J. Am. Chem. Soc.* **2009**, 131, 11195.
- (12) Mori, H.; Seino, H.; Hidai, M.; Mizobe, Y. *Angew. Chem., Int. Ed.* **2007**, 46, 5431.
- (13) (a) Kawaguchi, H.; Matsuo, T. *Angew. Chem., Int. Ed.* **2002**, 41, 2792. (b) Akagi, F.; Matsuo, T.; Kawaguchi, H. *Angew. Chem., Int. Ed.* **2007**, 46, 8778.
- (14) Hirotsu, M.; Fontaine, P. P.; Zavalij, P. Y.; Sita, L. R. *J. Am. Chem. Soc.* **2007**, 129, 12690.
- (15) Chatt, J.; Pearman, A. J.; Richards, R. L. *Nature* **1975**, 253, 39.
- (16) Shilov and co-workers reported the catalytic reduction of molecular dinitrogen into hydrazine. For recent reviews, see: (a) Shilov, A. E. *Coord. Chem. Rev.* **1995**, 144, 69. (b) Shilov, A. E. *Russ. Chem. Bull.* **2003**, 52, 2555.
- (17) Shiina, K. *J. Am. Chem. Soc.* **1972**, 94, 9266.
- (18) (a) Komori, K.; Oshita, H.; Mizobe, Y.; Hidai, M. *J. Am. Chem. Soc.* **1989**, 111, 1939. (b) Komori, K.; Sugiura, S.; Mizobe, Y.; Yamada, M.; Hidai, M. *Bull. Chem. Soc. Jpn.* **1989**, 62, 2953. (c) Oshita, H.; Mizobe, Y.; Hidai, M. *J. Organomet. Chem.* **1993**, 456, 213. (d) Mori, M. *J. Organomet. Chem.* **2004**, 689, 4210 and references therein.
- (19) (a) Yandulov, D. V.; Schrock, R. R. *Science* **2003**, 301, 79. (b) Ritleng, V.; Yandulov, D. V.; Weare, W. W.; Schrock, R. R.; Hock, A. S.; Davis, W. M. *J. Am. Chem. Soc.* **2004**, 126, 6150.
- (20) Cao, Z.; Zhou, Z.; Wan, H.; Zhang, Q. *Int. J. Quantum Chem.* **2005**, 103, 344.
- (21) Studt, F.; Tuzcek, F. *Angew. Chem., Int. Ed.* **2005**, 44, 5639.
- (22) (a) Le Guennic, B.; Kirchner, B.; Reiher, M. *Chem.—Eur. J.* **2005**, 11, 7448. (b) Reiher, M.; Le Guennic, B.; Kirchner, B. *Inorg. Chem.* **2005**, 44, 9640. (c) Schenk, S.; Le Guennic, B.; Kirchner, B.; Reiher, M. *Inorg. Chem.* **2008**, 47, 3634. (d) Schenk, S.; Reiher, M. *Inorg. Chem.* **2009**, 48, 1638.
- (23) Hölscher, M.; Leitner, W. *Eur. J. Inorg. Chem.* **2006**, 4407.
- (24) Magistrato, A.; Robertazzi, A.; Carloni, P. *J. Chem. Theory Comput.* **2007**, 3, 1708.
- (25) (a) Schrock, R. R. *Acc. Chem. Res.* **2005**, 38, 955. (b) Schrock, R. R. *Angew. Chem., Int. Ed.* **2008**, 47, 5512.
- (26) (a) Yuki, M.; Miyake, Y.; Nishibayashi, Y.; Wakiji, I.; Hidai, M. *Organometallics* **2008**, 27, 3947. (b) Yuki, M.; Midorikawa, T.; Miyake, Y.; Nishibayashi, Y. *Organometallics* **2009**, 28, 4741. (c) Yuki, M.; Miyake, Y.; Nishibayashi, Y. *Organometallics* **2009**, 28, 5821.
- (27) (a) Nishibayashi, Y.; Iwai, S.; Hidai, M. *Science* **1998**, 279, 506. (b) Nishibayashi, Y.; Takemoto, S.; Iwai, S.; Hidai, M. *Inorg. Chem.* **2000**, 39, 5946. (c) Nishibayashi, Y.; Saito, M.; Uemura, S.; Takekuma, S.; Takekuma, H.; Yoshida, Z. *Nature* **2004**, 428, 279.
- (28) (a) Tanaka, H.; Mori, H.; Seino, H.; Hidai, M.; Mizobe, Y.; Yoshizawa, K. *J. Am. Chem. Soc.* **2008**, 130, 9037. (b) Tanaka, H.; Ohsako, F.; Seino, H.; Mizobe, Y.; Yoshizawa, K. *Inorg. Chem.* **2010**, 49, 2464.
- (29) Tanaka, H.; Shiota, Y.; Matsuo, T.; Kawaguchi, H.; Yoshizawa, K. *Inorg. Chem.* **2009**, 48, 3875.
- (30) Frisch, M. J.; et al. *Gaussian 09*, revision A.01; Gaussian, Inc.: Wallingford CT, 2009.
- (31) (a) Becke, A. D. *Phys. Rev. A* **1988**, 38, 3098. (b) Becke, A. D. *J. Chem. Phys.* **1993**, 98, 5648. (c) Lee, C.; Yang, W.; Parr, R. G. *Phys. Rev. B* **1988**, 37, 785. (d) Stephens, P. J.; Devlin, F. J.; Chabalowski, C. F.; Frisch, M. J. *J. Phys. Chem.* **1994**, 98, 11623.
- (32) (a) Ditchfield, R.; Hehre, W. J.; Pople, J. A. *J. Chem. Phys.* **1971**, 54, 724. (b) Hehre, W. J.; Ditchfield, R.; Pople, J. A. *J. Chem. Phys.* **1972**, 56, 2257. (c) Hariharan, P. C.; Pople, J. A. *Theor. Chim. Acta* **1973**, 28, 213. (d) Clark, T.; Chandrasekhar, J.; Spitznagel, G. W.; Schleyer, P. v. R. *J. Comput. Chem.* **1983**, 4, 294. (e) Francl, M. M.; Pietro, W. J.; Hehre, W. J.; Binkley, J. S.; Gordon, M. S.; DeFrees, D. J.; Pople, J. A. *J. Chem. Phys.* **1982**, 77, 3654. (f) Hay, P. J.; Wadt, W. R. *J. Chem. Phys.* **1985**, 82, 299.
- (33) Tomasi, J.; Mennucci, B.; Cammi, R. *Chem. Rev.* **2005**, 105, 2999.
- (34) Hidai, M.; Mizobe, Y. *Chem. Rev.* **1995**, 95, 1115.